CrossMark

# Metabo-lipidomics of Fibroblasts and Mitochondrial-Endoplasmic Reticulum Extracts from ALS Patients Shows Alterations in Purine, Pyrimidine, Energetic, and Phospholipid Metabolisms

Charlotte Veyrat-Durebex[1,2,3] · Céline Bris[1,2] · Philippe Codron[2,4] · Cinzia Bocca[2] · Stéphanie Chupin[1] · Philippe Corcia[5,6,7] · Patrick Vourc'h[3,5] · Rudolf Hergesheimer[5] · Julien Cassereau[2,4] · Benoit Funalot[7] · Christian R Andres[3,5] · Guy Lenaers[2] · Philippe Couratier[7] · Pascal Reynier[1,2] · Hélène Blasco[2,3,5]

## Abstract

Amyotrophic lateral sclerosis (ALS) is characterized by a wide metabolic remodeling, as shown by recent metabolomics and lipidomics studies performed in samples from patient cohorts and experimental animal models. Here, we explored the metabolome and lipidome of fibroblasts from sporadic ALS patients ($n = 13$) comparatively to age- and sex-matched controls ($n = 11$), and the subcellular fraction containing the mitochondria and endoplasmic reticulum (mito-ER), given that mitochondrial dysfunctions and ER stress are important features of ALS patho-mechanisms. We also assessed the mitochondrial oxidative respiration and the mitochondrial genomic (mtDNA) sequence, although without yielding significant differences. Compared to controls, ALS fibroblasts did not exhibit a mitochondrial respiration defect nor an increased proportion of mitochondrial DNA mutations. In addition, non-targeted metabolomics and lipidomics analyses identified 124 and 127 metabolites, and 328 and 220 lipids in whole cells and the mito-ER fractions, respectively, along with partial least-squares–discriminant analysis (PLS-DA) models being systematically highly predictive of the disease. The most discriminant metabolomic features were the alteration of purine, pyrimidine, and energetic metabolisms, suggestive of oxidative stress and of pro-inflammatory status. The most important lipidomic feature in the mito-ER fraction was the disturbance of phosphatidylcholine PC (36:4p) levels, which we had previously reported in the cerebrospinal fluid of ALS patients and in the brain from an ALS mouse model. Thus, our results reveal that fibroblasts from sporadic ALS patients share common metabolic remodeling, consistent with other metabolic studies performed in ALS, opening perspectives for further exploration in this cellular model in ALS.

**Keywords** Amyotrophic lateral sclerosis · Metabolomics · Lipidomics · Fibroblasts · Mitochondria · Oxidative stress

✉ Charlotte Veyrat-Durebex
charlotte.veyrat@live.fr

✉ Hélène Blasco
helene.blasco@univ-tours.fr

1 Département de Biochimie et Génétique, CHU d'Angers, Angers, France

2 Unité Mixte de Recherche MITOVASC, CNRS 6015-INSERM 1083, Université d'Angers, Angers, France

3 Laboratoire de Biochimie et Biologie Moléculaire, CHRU Hôpital Bretonneau, 2, Bd Tonnellé, 37044 Tours, France

4 Centre de Ressources et de Compétences SLA, Service de Neurologie, CHU Angers, Angers, France

5 Université de Tours, Inserm U1253, Tours, France

6 Centre de Référence SLA, Service de Neurologie, CHRU Bretonneau, Tours, France

7 Fédération des CRCSLA Tours et Limoges, LITORALS, Tours, France

# Introduction

Amyotrophic lateral sclerosis (ALS) is a fatal, neurodegenerative disease causing the progressive loss of motor neurons, and death only 3 to 5 years after diagnosis [1]. There is no cure for ALS, and the only two drugs available to date are riluzole and, more recently, edaravone that present limited efficacy. The pathophysiology of ALS includes glutamatergic excitotoxicity, oxidative stress, mitochondrial dysfunctions, abnormal protein aggregations, and neuroinflammation [2–5]. Nevertheless, these mechanisms and their interconnectedness are still only partially understood. Thus, new "omics" strategies further integrating these patho-mechanisms and revealing undescribed targets remain of utmost importance for the development of ALS treatments. Metabolic alterations have been largely described in ALS through targeted and untargeted approaches in the body fluids and tissues of patients, as well as in animal and cellular models [6].

Patient fibroblasts, often used in the exploration of mitochondrial diseases, have proven to be of use to understand ALS etiology, but so far they have not been analyzed by metabolomics. In ALS, skin fibroblasts have shown to display numerous abnormalities found in motor neurons [7] suggesting that these apparently unaffected cells may share common pathogenic pathways with motor neurons. Moreover, human fibroblast cultures have demonstrated that they are an accessible model to study the function of mitochondrial metabolism in ALS [8]. Fibroblasts of sporadic ALS (sALS) patients display an increased, uncoupled mitochondrial respiration and glycolytic rate compared to same-age control fibroblasts [9]. Similar defects in mitochondrial respiration with increased glycolytic flux were observed in fibroblasts from patients carrying *SOD1* pathogenic variants [10]. A higher mitochondrial membrane potential associated to decreased mitochondrial content was observed in ALS fibroblasts, and the correlation with age at diagnosis offers hope in discovering potential ALS biomarkers [11]. A recent study showed that fibroblasts from patients affected with sALS, primary lateral sclerosis, or familial ALS related to *C9ORF72* expansion repeats, were hyper-metabolic in order to counteract the energetic impairment [7]. This highlights the relevance of mitochondrial membrane potential, respiration, glycolysis, and ATP content to the classification of patients. Mitochondrial function also depends on its structure, including membrane composition, and the cellular environment. According to the link of polyunsaturated fatty acids with inflammatory mediators, and with the breakdown of cell membranes during neuronal degeneration [12, 13], we hypothesize that specific lipid and metabolic profiles may characterize the ALS pathologic condition. Mitochondria and ER are physically closely related by the mitochondria-associated membranes (MAM) that constitute the sites of lipids, calcium, and proteins transferred from the ER towards mitochondria, with a crucial regulatory role in cell homeostasis. MAM display a key role in the mitochondrial fission, apoptosis, and ROS generation. Defects in lipid metabolism observed at the MAM contact sites might be involved in pathophysiology of various conditions such as neurodegenerative or metabolic diseases [14], especially in ALS [15]. Since endoplasmic reticulum (ER) stress has been observed in familial and sporadic ALS [16, 17], the association between mitochondrial and ER defects in ALS led us to specifically explore this subcellular fraction, using a quick extraction protocol for metabolomics and lipidomics analyses [18]. Indeed, recent studies reported mitochondrial lipidome [19–22], but the long procedures used to isolate mitochondria are incompatible with metabolomics analyses due to the risk of metabolite degradation.

Here, we report metabolomic and lipidomic explorations of fibroblasts from ALS patients, both on whole cells and their mitochondrial-endoplasmic reticulum (mito-ER) fraction, and correlate these data to the functional assessment of oxidative phosphorylation (OXPHOS) and complete mitochondrial DNA sequencing, in order to unravel the metabolic disturbances through a multi-omics approach and to specify the alterations of the mitochondria-ER fraction.

# Materials and Methods

## Patients

Skin fibroblasts were obtained from 13 sporadic ALS patients diagnosed and followed in two French ALS reference centers: Angers and Limoges University Hospitals. ALS patients satisfied the diagnostic criteria of "probable" or "definite" symptoms as defined by the El Escorial workshop [23]. Information on diagnosis, gender, current age, site of onset, diagnostic delay, and age at onset were obtained for each patient. We also collected the parameters of disease progression, such as the revised ALS functional rating scale (ALSFRS-r), the forced vital capacity (FVC), and the body mass index (BMI) at the time of diagnosis.

Control fibroblasts from 11 gender- and age-matched healthy subjects were selected in the Biological Resource Center (Centre de Ressource Biologique CRB) from the hospital of Angers. All the participants in this current study provided their informed consent for the use of their fibroblasts for research. The ethic committees of the Centre for Human Research of Angers and Limoges Hospitals approved the study and the consent process (no 2016/36, 2016-A01425-46).

## Fibroblast Culture

Human fibroblasts were cultured in a medium consisting of two-third Dulbecco's modified Eagle medium with nutrient mixture F12 (DMEM-F12, PAN Biotech), one-third AmnioMAX™

(Gibco, Invitrogen) supplemented with 10% fetal bovine serum (PAN Biotech) at 37 °C and 5% $CO_2$. To avoid artifacts due to senescence, all experiments were conducted on fibroblast cultures between the 6th and the 15th passages [24].

A schematic flowchart of experiments is presented in Fig. 1.

## OXPHOS Exploration

The mitochondrial respiration rates were measured using a two-channel, high-resolution oxygraph respirometer (Oroboros, Innsbruck, Austria) in a minimum of three replicates. Cells were grown to 70–90% confluency and approximatively three million cells in DMEM-F12 were used for analysis. Firstly, the basal respiration was measured (i.e., routine oxygen consumption rate (OCR)). Secondly, the non-phosphorylating respiration (proton leak) was evaluated by adding an ATP synthase inhibitor, oligomycin (4 μg/mL) (Oligomycin OCR). Then, maximal capacity of cellular respiration was assessed by adding successive doses of FCCP (p-trifluoromethoxy-carbonyl-cyanide-phenyl hydrazine). Finally, we used an inhibitor of mitochondrial complex III, antimycin (2 μg/mL) to evaluate the non-mitochondrial oxygen consumption. The respiration capacity rate (RCR) was calculated as the ratio between the maximal capacity of respiration and the non-phosphorylating respiration. The phosphorylating RCR was obtained by the subtraction of non-phosphorylating respiration to basal respiration divided by the maximal capacity of respiration. We measured the concentration of proteins of each sample to normalize oxygen uptake between samples.

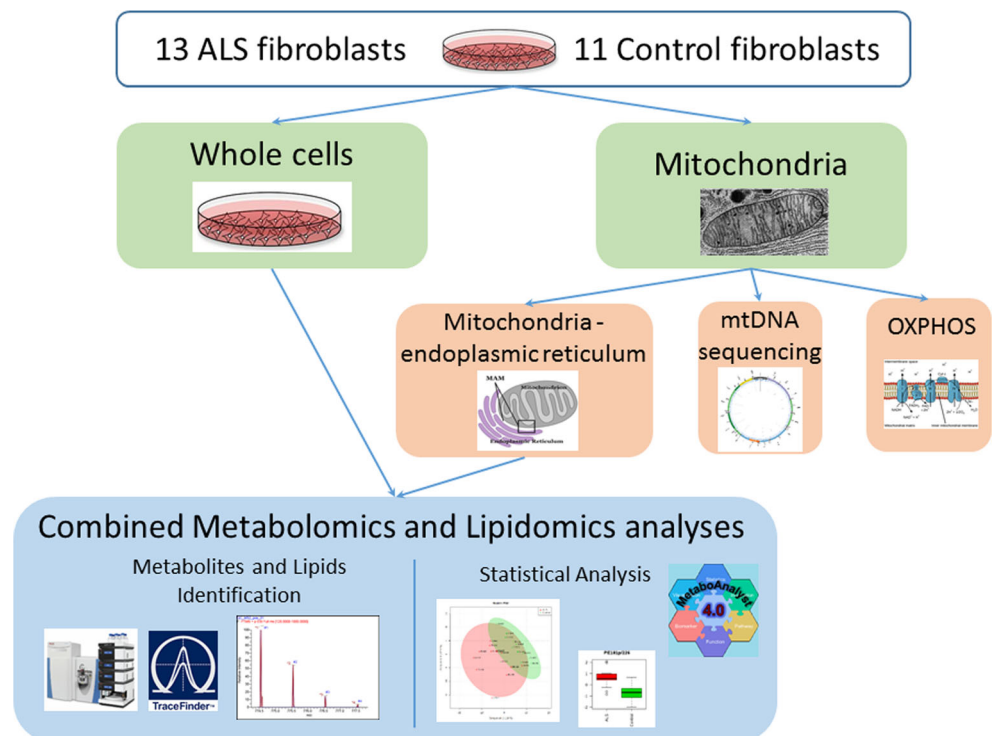## Metabolomic and Lipidomic Analyses

### Whole Cell Extraction

Samples were extracted as previously described [25]. After medium removal, the cellular monolayer was rinsed twice with an aqueous solution containing 0.22% NaCl before being quenched with cold methanol for metabolomic analysis and with a cold mixture of ammonium bicarbonate at 155 mM and methanol (67.7/32.3) for lipidomics. The cell suspension (4 million cells) obtained after mechanical scraping was then collected in aliquots of one million cells and stored at −80 °C until analysis.

### Mitochondria and Endoplasmic Reticulum (Mito-ER) Extraction

The mitochondria plus endoplasmic reticulum (mito-ER) fraction was extracted as previously described [18]. Briefly, cell lysis of pellets containing 10 million cells was achieved in a Precellys24® homogenizer (Bertin Instruments) using 1 cycle of grinding 5 s at 2500 rpm at 4 °C. Then differential centrifugations were performed for mito-ER purification.

**Fig. 1** Flowchart summarizing the global methodology

## Metabolomics and Lipidomics

Metabolomics and lipidomics protocols and analytical systems have been detailed and recently published [18, 25]. HRMS system was based on UPLC Ultimate 3000 system (Dionex) coupled to a Q-Exactive Mass Spectrometer (ThermoFisher Scientific, Bremen, Germany) using electrospray ionization (positive and negative Electrospray Ionization (ESI+ and ESI-)). Quality controls (QC) were analyzed regularly on the plate (every 8 samples) to ensure the stability of the mass system over time. Accordingly, peaks that had high variability (coefficient of variation > 30%) were excluded from further analysis. Metabolites were identified at level 1 and lipids at level 2 according to the level of compound identification process [26].

## Mitochondrial DNA Sequencing

Total DNA was extracted from patient fibroblasts using the Nucleospin® tissue Kit (Macherey-Nagel®) and the EZ1 DNA extraction automate (Qiagen) according to the manufacturer's recommendations. Whole mitochondrial genome (mtDNA) was sequenced using Ion Proton high-throughput sequencing platform and analyzed as previously described [27]. Variants were filtered using the following criteria: at least three callers predicting the variant, strand bias between 0.25–0.75, and a minimum mtDNA heteroplasmy level of 2%. Putative variants were visualized on Integrative Genome Viewer [28] to avoid artifacts. Variant prioritization relies on databases, i.e., Mitomap [29], HmtDB [30], Mamit [31], and prediction tools, i.e., MitImpact [32] and MitoTip [33]. Variant heteroplasmy was considered as low under 30%, medium between 30% and 70% and high between 70% and 95%, and above 95% variants were considered as homoplasmic. Mitochondrial haplogroups were determined using Phy-Mer [34]. Structural mtDNA rearrangements were analyzed trough a home-made tool based on soft-clipping.

## Statistical Analysis

We performed both multivariate and univariate analyses using Metaboanalyst, version 3.0 (http://www.metaboanalyst.ca) for metabolomics and lipidomics data. Classification method was based on Partial Least-Squares Discriminant Analysis (PLS-DA). Values of variable importance in projection (VIP) represent the importance of the compound (metabolite/lipid) for the PLS-DA models. The score plots show the classified samples and the loadings characterize the relation between the Y and X variables (metabolites, lipids). Metaboanalyst modeling includes leave-one-out cross-validation (LOOCV). We retained the 15 most discriminant compounds based on the VIP to explore pathways. To attest the relevance of these selected compounds, the quality of the model built with these selected discriminant metabolites was assessed by prediction accuracy and permutation test (set permutation $n = 100$). The performance measures of the permutated data usually form a normal distribution and if the performance score of the original data lies outside the distribution, then the results are considered significant.

The univariate analysis of metabolites and lipids levels was based on the fold-change values and the threshold of significance after non-parametric Wilcoxon test, using Benjamini and Hochberg correction for multiple tests.

Non-parametric Wilcoxon test was used to compare clinical data, oxygen consumption rate, and mtDNA sequencing data between ALS and controls.

## Pathway Analysis

We used KEGG pathway database (http://www.genome.jp/kegg/pathway.html) on Metaboanalyst tool to discuss the highlighted metabolic pathways. To focus on the most relevant data, we highlighted only the pathways that had significant Holm $p$ and $a$ pathway impact > 0.05. The pathway impact value is the cumulative percentage from the matched metabolite nodes.

## Results

### Patients

No statistical difference was found regarding age and gender between the 13 ALS and 11 control subjects. The mean age at onset of ALS was $60.5 \pm 9.9$ years, and percentage of females was 38.5% (Table 1). About 77% of ALS patients had a spinal onset. None of these patients carried mutations or expansions in *SOD1*, *TARDBP*, *FUS*, or *C9ORF72* genes. Characteristics of ALS patients at diagnosis defined by BMI, FVC, and ALSFRS-r score were as follows: $22.8 \pm 3.2$ kg/m$^2$, $81.6 \pm 18.9\%$, and $38.2 \pm 4.5$, respectively. There was no significant difference in mean passage number between ALS and control fibroblast cultures used for analyses (data not shown).

### Mitochondrial Exploration

#### OXPHOS Analysis

The OXPHOS analysis revealed no differences in basal and maximal respiration between ALS and control fibroblasts. We did not detect any difference in respiratory capacity rate (RCR) or in phosphorylating RCR (Table 2).

**Table 1** Clinical characteristics of ALS patients and controls. SD = standard deviation

|  | ALS patients mean ± SD | Controls mean ± SD | *p* value |
|---|---|---|---|
| Age (mean ± SD) | 60.5 ± 9.9 | 54.3 ± 11.4 | 0.12 |
| Gender (% of female) | 38.5 | 33.3 | 1 |
| Age of onset (years) | 59.4 ± 9.1 |  |  |
| BMI (kg/m$^2$) | 22.8 ± 3.2 |  |  |
| FVC (%) | 81.6 ± 18.9 |  |  |
| ALSFRS-R | 38.2 ± 4.5 |  |  |

## mtDNA Sequencing

mtDNA from 12 ALS and 11 control fibroblasts was sequenced, while one ALS sample could not be processed. We did not identify any large-scale rearrangement in patients or controls. Considering all samples together, 505 punctual variants were found, among which 124 were unrelated to the mitochondrial haplogroups (combinations of polymorphisms retracing human evolution), including 66 heteroplasmic variants. Among the non-haplogroup variants, 32 (25.8%) occurred in the D-Loop, the non-coding region controlling replication and transcription of mtDNA, 69 (55.6%) were located in polypeptide-coding regions, 10 (8.1%) in tRNA genes, and 13 (10.5%) in rRNA genes. Figure 2 shows the repartitioning of these variants in ALS and control fibroblasts. Twenty-eight (42.4%) of the heteroplasmic variants were recognized as non-pathogenic variants, nine (13.6%) were associated with clinical phenotypes, and 29 (44%) were not reported in all mitochondrial databases. The level of heteroplasmy was considered to be low for 61 (63.5%) variants and medium for five of them (15.4%).

Statistical comparison between the ALS and control groups did not disclose difference between the total number of variants, the number of non-haplogroup variants, or the number of variants in the different mtDNA genes (Table 2). Of note, the mean level of heteroplasmic variants per ALS patient was 3.4, while it was 2.3 per control, but this difference was not significant. Interestingly, only ALS patients had mtDNA variants with medium levels of heteroplasmy among the non-haplogroup variants ($p = 0.0179$) (Table 3). We did not

observe any difference in the number of pathogenic variants between ALS and controls. Reported pathogenic variants found in the ALS and control fibroblasts are reported in supplementary Table S1.

## Metabolomic and Lipidomic Signatures of ALS Fibroblasts

We detected and identified 124 and 127 metabolites and 328 and 220 complex lipids in fibroblasts and mito-ER extracts, respectively (Supplementary Tables S2 and S3).

The PLS-DA model from metabolomic data on total fibroblasts revealed an excellent discrimination between ALS patients and controls (75% accuracy, *p* value of permutation test: 0.01) (Fig. 3a). The 15 most discriminant metabolites were attributed with VIP scores higher than 1 and are presented in Fig. 3b. Mito-ER metabolomics correctly distinguished ALS patients and controls (accuracy: 62.5%, *p* value of permutation test: 0.1) (Fig. 3d). VIP scores of the 15 most discriminant metabolites were higher than 1.5, and 3 of them were significant after univariate analysis: inosine, guanosine, and guanine ($p < 0.03$ and FC > 1.5) (Fig. 3e).

Whole cell and mito-ER lipidomics also displayed correct discriminations between ALS and control subjects (64% and 50% accuracies, *p* values of permutation tests 0.17 and 0.75, respectively). In these two non-optimized models, the 15 most discriminant lipids had VIP scores higher than two (Fig. 4b and d). Optimized PLS-DA models using only the 15 top VIP metabolites improved the discriminations between ALS and controls in both whole cells and mito-ER lipidomic data, with

**Table 2** Exploration of oxidative phosphorylation of ALS and control fibroblasts. SD = standard deviation

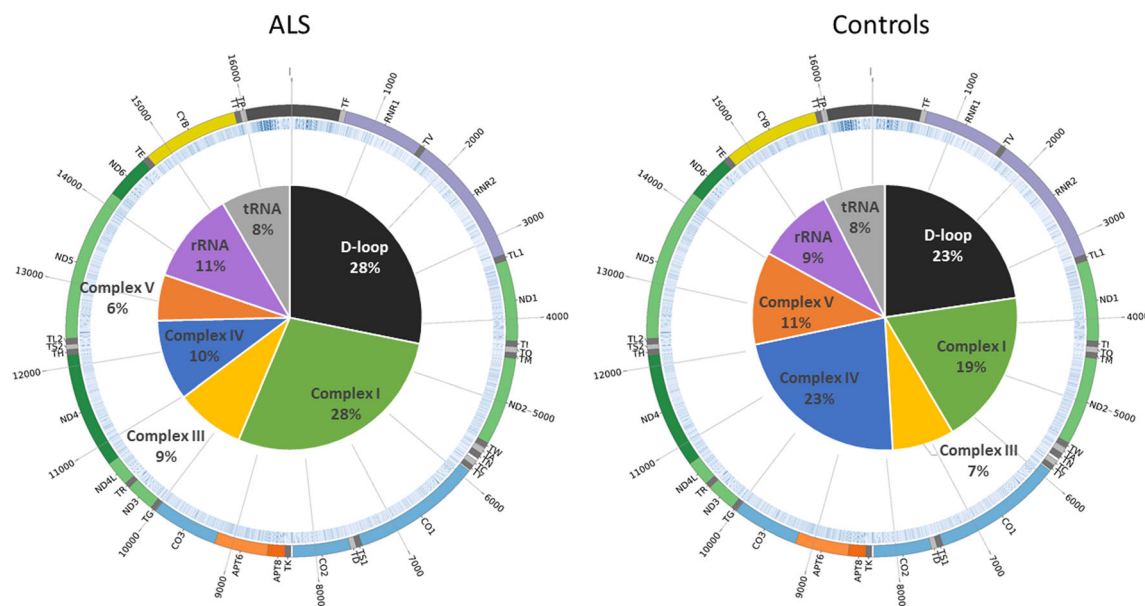| Oxygen consumption rate (OCR) (pmol O$_2$/min) | ALS patients mean ± SD | Controls mean ± SD | *p* value |
|---|---|---|---|
| Routine OCR | 152.7 ± 27.6 | 160.9 ± 31.1 | 0.5 |
| Oligomycin OCR | 46.1 ± 7.7 | 48.9 ± 7.5 | 0.5 |
| Maximal capacity of respiration | 399.3 ± 82.4 | 406.5 ± 97.2 | 0.88 |
| Respiration capacity rate (RCR) | 3.5 ± 0.8 | 3.4 ± 0.5 | 0.5 |
| Phosphorylating RCR | 0.009 ± 0.002 | 0.009 ± 0.001 | 0.93 |

**Fig. 2** Circos representing mtDNA sequence (black: D-loop; gray: tRNA genes; purple: rRNA genes; green: complex I genes; yellow: complex III genes; blue: complex IV genes; orange: complex V genes). The pie chart in the center of each circos (ALS and controls) shows the repartition of heteroplasmic variants on the mtDNA

80% and 83% accuracy, and 0.03 and 0.08 for $p$ values of permutation tests in whole cells and mito-ER extracts, respectively (Fig. 4a and c). Univariate analysis did not reveal significant variation in lipid concentrations.

## Metabolomic Findings

Using the "pathway analysis" module of the MetaboAnalyst software, we explored the pathways involved in the

**Table 3** Summary of mtDNA variants found in ALS and control fibroblasts. *p value < 0.05 was considered as significant

| | mtDNA | ALS | | Control | | $p$ value |
|---|---|---|---|---|---|---|
| | Total sites | Total | Per individual ($n = 12$) | total | Per individual ($n = 11$) | |
| Total variants | 16,569 | 264 | 22.0 | 241 | 21.9 | 0.9508 |
| Total non-haplogroup (HP) variants | 16,569 | 71 | 5.9 | 53 | 4.8 | 0.5536 |
| Total homoplasmic variants non HP | 16,569 | 30 | 2.5 | 28 | 2.5 | 0.9000 |
| Total heteroplamic variants non HP | 16,569 | 41 | 3.4 | 25 | 2.3 | 0.4330 |
| Variants non HP location | | | | | | |
| D-loop | 1121 | 20 | 1.7 | 12 | 1.1 | 0.2624 |
| All coding | 15,409 | 51 | 4.3 | 41 | 3.7 | 0.9255 |
| Complex I | 6349 | 20 | 1.7 | 10 | 0.9 | 0.1829 |
| Complex III | 1141 | 6 | 0.5 | 4 | 0.4 | 0.3886 |
| Complex IV | 3010 | 7 | 0.6 | 12 | 1.1 | 0.2018 |
| Complex V | 888 | 4 | 0.3 | 6 | 0.5 | 0.4724 |
| rRNA | 2513 | 8 | 0.7 | 5 | 0.5 | 0.8558 |
| tRNA | 1508 | 6 | 0.5 | 4 | 0.4 | 0.8835 |
| Type of variants | | | | | | |
| Reported pathogenic variants | 16,569 | 6 | 0.5 | 3 | 0.3 | 0.2358 |
| Non reported in DB variants | 16,569 | 17 | 1.4 | 12 | 1.1 | 0.5524 |
| Heteroplasmy | | | | | | |
| Low (1–30%) | 16,569 | 36 | 3.0 | 25 | 2.3 | 0.7018 |
| Medium (30–70%) | 16,569 | 5 | 0.4 | 0 | 0.0 | 0.0179 * |
| High (70–95%) | 16,569 | 0 | 0.0 | 0 | 0.0 | |
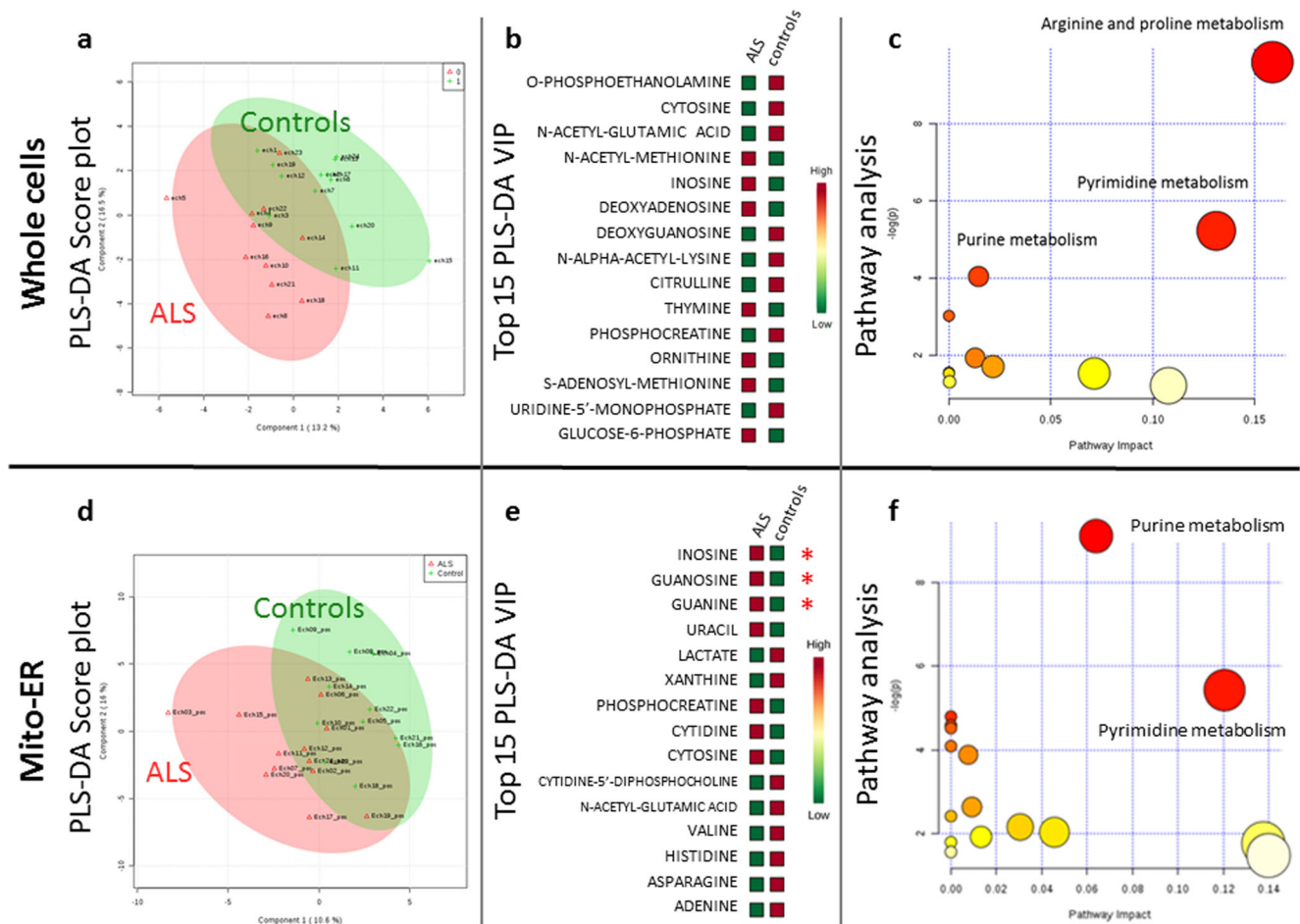
**Fig. 3** Metabolomic data analyses of whole cells and mito-ER fraction. A. Optimized PLS-DA 2D-score plot from metabolomic whole cells data (red triangle: ALS samples; green cross: control samples) showing discrimination between the two groups. B. List of the top 15 VIP (variable importance in projection) from non-optimized PLS-DA model from metabolomic whole cells data. C. Results of pathway analysis including the top 15 VIP metabolites of whole cells PLS-DA model (using MetaboAnalyst module). D. Optimized PLS-DA 2D-score plot from metabolomic mito-ER data (red triangle: ALS samples; green cross: control samples) showing the discrimination between the two groups. E. List of the top 15 VIP (variable importance in projection) from non-optimized PLS-DA model from metabolomic mito-ER data (red stars show metabolites significant in univariate analysis with $p < 0.05$ and fold change > 1.2). F. Results of pathway analysis including top 15 VIP metabolites of mito-ER PLS-DA model (using MetaboAnalyst module)

metabolomic signatures of ALS whole fibroblasts and mito-ER extracts. The main pathways involving the 15 most discriminant metabolites identified with robustness in ALS fibroblasts were arginine and proline metabolism, pyrimidine, and purine metabolism (Fig. 3c). The pathway analysis of the metabolomic signature of ALS mito-ER notably underscored the involvement of purine and pyrimidine metabolism, as well (Fig. 3f).

The global analysis of metabolic disturbances based on fibroblasts and their mito-ER fraction disclosed modifications of purine (adenine and guanine) and pyrimidine bases (cytosine, uracil, and thymine), and various nucleosides and their derivatives (inosine, guanosine, cytidine, deoxyadenosine, deoxyguanosine, uridine-5′-monophosphate, and cytidine-5′-diphosphocholine). We also observed a decrease in xanthine in the mito-ER fraction.

Metabolomic signatures also highlighted several compounds involved in energy metabolism. Indeed, we noticed variations in glucose-6-phosphate levels in ALS whole fibroblasts and in lactate levels in the mito-ER fraction. This was associated with a modification of the phosphocreatine levels in both ALS fibroblasts and mito-ER fractions.

## Lipidomic Findings

We found a reduction in several ceramide concentrations in the ALS mito-ER fraction and a gain in sphingolipid (SM) levels in ALS whole cells (Fig. 4). Lipidomic profiles of ALS fibroblasts highlighted modifications in phosphatidylcholine (PC) and phosphatidylethanolamine (PE) levels, both in whole cell and mito-ER extracts (Fig. 4). Interestingly, we observed several plasmalogen species among the VIP
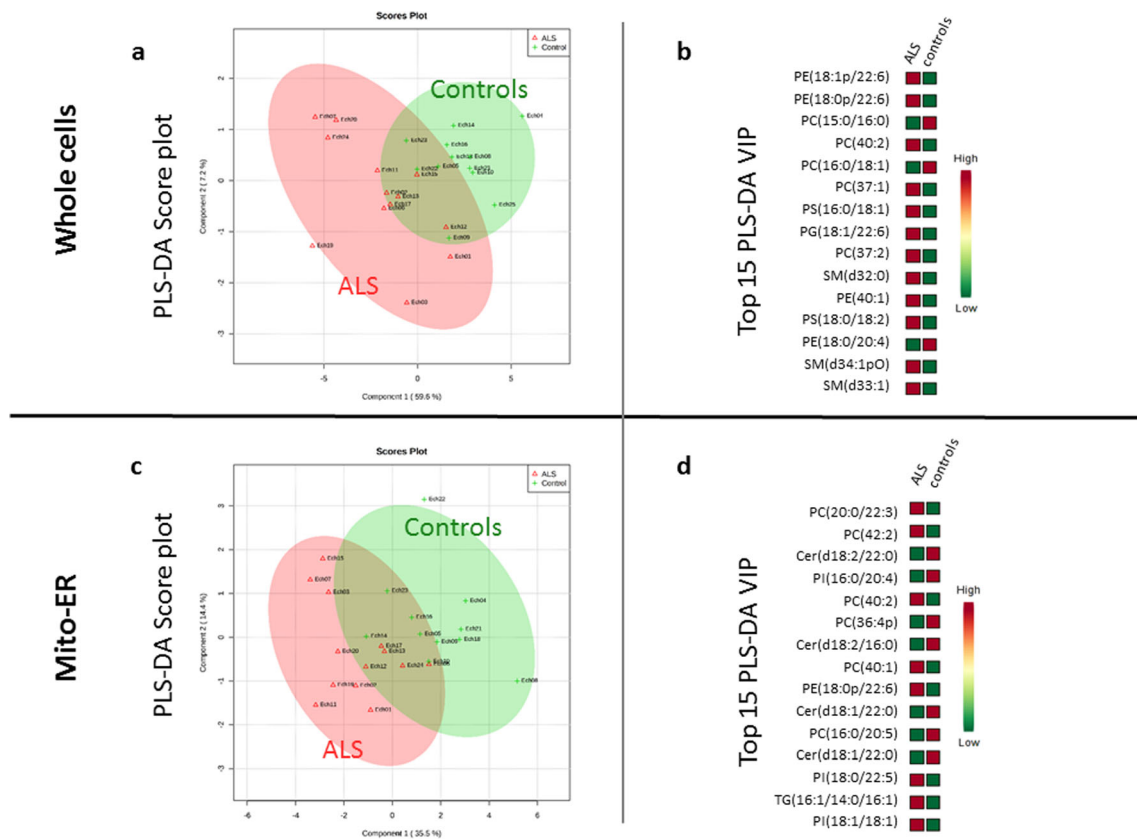
**Fig. 4** Lipidomic data analyses of whole cells and mito-ER fraction. A. Optimized PLS-DA 2D-score plot from lipidomic whole cells data (red triangle: ALS samples; green cross: control samples) showing discrimination between the two groups. B. List of the top 15 VIP (variable importance in projection) from non-optimized PLS-DA model from lipidomic whole cells data. C. Optimized PLS-DA 2D-score plot from lipidomic mito-ER data (red triangle: ALS samples; green cross: control samples) showing discrimination between the two groups. D. List of the top 15 VIP (variable importance in projection) from non-optimized PLS-DA model from lipidomic mito-ER data

metabolites of both models—PE plasmalogen (PEp) in the whole cells with PE(18:1p/22:6) and PE(18:0p/22:6); and PE(18:0p/22:6) and PC(36:4p) in the mito-ER extract.

## Discussion

This study provides the first report of a multi-omics profiling on sporadic ALS fibroblasts, both at the whole cell and mito-ER subcellular levels, complemented by OXPHOS measurement and mtDNA complete sequencing.

### Multiple Implications of the Purine and Pyrimidine Metabolisms in Oxidative Stress and Inflammation in ALS

The alterations of purine and pyrimidine metabolisms recognized in this study are convergent with data from a previous study that we performed on rodent motor neurons and astrocytes [35], placing these pathways at the core of oxidative stress and inflammatory mechanisms observed in ALS [36]. Purine catabolism leads to the production of xanthine, which

is converted to uric acid by xanthine oxidase, finally producing reactive oxygen species (ROS) [37]. This is consistent with the increase in uric acid and ROS production found in ALS patients; we also found that xanthine levels were lower in the mito-ER samples compared to the controls, possibly signifying an augmented depletion due to uric acid production. We did not highlight significant differences in uric acid levels in our study ($p = 0.6635$), but we had a small cohort reducing statistical power. Uric acid has numerous roles in cell homeostasis, and its function in oxidative stress, especially increased in ALS, may explain this finding. Indeed, uric acid concentrations increase in response to oxidative stress and act as a scavenger of singlet oxygen and hydroxyl radicals [38]. Therefore, uric acid acts as either an antioxidant (especially in plasma) or a pro-oxidant in cells [39], suggesting a role in oxidative stress as a primary phenomenon or as a neuroprotective effect [40]. Interestingly, multiple studies have displayed support for the latter. It has been shown that uric acid modulates neuroinflammation by decreasing the serum levels of IL-1β, IL-6, and TNF-α in Parkinson's disease murine models [41]. Furthermore, primary astrocyte-conditioned medium provides a neuroprotective effect against both $H_2O_2$-

induced and SOD1^{G93A} astrocyte-induced oxidative stress in NSC-34 cells, when the normal or mutant astrocytes are first treated with uric acid [42].

## Disturbances in Energy Metabolism in ALS

An imbalance in ATP production and consumption could explain an increased rate of purine catabolism with consequent modifications in purine end-product levels, as xanthine and inosine observed here. A recent study showed that multiple sclerosis is characterized by perturbations in energy metabolism, leading to significant changes in the serum profiles of compounds directly (purines) or indirectly (creatinine, lactate, and pyrimidines) connected to ATP homeostasis [43]. Our findings are consistent with the results of this study, since ALS also involves metabolic imbalances. In this respect, we also noticed modified amounts of phosphocreatine, which mediates ADP phosphorylation and could be a response to energetic impairment. It is also known to stabilize mitochondrial membranes by binding phospholipids [44]. In addition, phosphocreatine has neuroprotective effects against oxidative stress and mitochondrial dysfunction [45]. As in cancer cells, significant levels of aerobic glycolysis, the so-called Warburg Effect, have been documented in ALS due to the overactivation of the WNT/β-catenin pathway [46]. This is supported by the observation of modifications in the concentration of glucose-6-phosphate, a glycolytic intermediate, related with variations in lactate levels. All these findings support the alteration of the energy metabolism in ALS, associated with oxidative imbalance and inflammation. As explained by Lu et al., the reported concentrations of cellular ATP are notoriously inconsistent because of incomplete quenching and incomplete extraction for mass spectrometry method. Enzyme assays reveal that ATP concentration is more reflective of overall purine abundance than cellular energetics [47]. Thus, these results also lead us to program further explorations of energy metabolism through the measurement of glycolytic and mitochondrial production of ATP.

## Involvement of Phospholipids and Sphingomyelins in Neuroprotective Mechanisms

Lipidomic results further suggest perturbations in the oxidative mechanism and inflammation. Indeed, higher concentrations of PCs observed in ALS fibroblasts may stimulate the metabolic activity of phospholipase A2 (PLA2), resulting in an increased production of lipid mediators, such as eicosanoids that promote inflammation and are considered to play a role in ALS pathophysiology [48, 49].

Three plasmalogen species, corresponding to phospholipids (PL) having an ether bond between fatty acids and glycerol, were discriminants between ALS and control fibroblasts: (PE(18:1p/22:6), PE(18:0p/22:6), PC(36:4p)). Plasmalogens

are important components of myelin, subcellular membranes as the mitochondrial membranes, and the membranes of secretory granules. The main functions of plasmalogens are the generation of lipid second messengers and the conservation of membrane integrity. Plasmalogens, which terminate lipid oxidation and protect ROS-vulnerable myelin, are considered to act as endogenous antioxidants [50, 51], which, in the context of ALS, can prevent the oxidation of polyunsaturated fatty acids and other lipids.

Our results further disclosed higher levels of sphingomyelins (SM) in ALS fibroblasts, associated with lower ceramide (Cer) levels in mito-ER fractions. Classically, ceramides are synthesized using serine in the ER then are converted to SM. These results are consistent with the lipidomic signature of the cerebrospinal fluid (CSF) from ALS patients [52], with the higher levels of ceramides and glucosylceramides found in the spinal cord of ALS patients and in ALS mouse model [53], and with the fact that ceramides have been associated with apoptosis in response to cytotoxic humoral factors [54]. Indeed, the accumulation of ceramide-derived agents may be protective by reducing ceramide synthesis and increasing the entry of ceramides into the CerG1 pathway, thus limiting the direct toxic effect on motor neurons [53]. Higher ceramide and downstream glycosphingolipid levels have also been reported in the muscle of an ALS mouse model, as well as in other mice after muscle injury [55]. Taken together, these findings clearly show a perturbation of the glycosphingolipid metabolism in ALS fibroblasts. These results open perspectives of deeply studying ER function in ALS.

The identification of the fatty acid chain 22:6 in the discriminant phospholipids, i.e., (PE(18:0p/22:6), PE(18:1p/22:6), PG(18:1/22:6)), corresponds to docosahexaenoic acid (DHA), an omega-3 polyunsaturated fatty acid (n-3 PUFA) that is involved in the maintenance of neuronal membranes, signal transduction, neuronal differentiation, neurogenesis, and protection against synaptic loss and spinal cord injury [56]. Moreover, some authors have highlighted the significant increase in DHA in the frontal cortex of ALS patients [17]. This phenomenon may be considered as a potentially defensive response of the nervous tissue to brain ischemia and Alzheimer's disease [57], or as an inflammatory process via the production of n-3-derived anti-inflammatory resolvins and docosatrienes by the brain cortex [58]. We also recently reported discriminant phospholipids containing DHA in the lipidomic signature of ALS cerebrospinal fluids [52].

## Mitochondrial Instability as a Protective Mechanism?

The assessment of OXPHOS capacities revealed that there was no difference in cellular respiration between ALS and control fibroblasts. MtDNA sequences of ALS fibroblasts were similar to those of controls in terms of total number of

variants per sample, frequency of mtDNA variants, type of mtDNA variants, and patterns of distribution. Nevertheless, we found that ALS cells exhibited higher levels of heteroplasmy, which may attest to a higher mtDNA instability. We could note that reported pathogenic variants found in ALS fibroblasts are associated with Parkinson's disease, dystonia and myopathy, hypertrophic cardiomyopathy, and Leber Hereditary Optic Neuropathy (LHON) mitochondrial diseases. Despite the absence of obvious mtDNA alteration in ALS fibroblasts, mitochondrial dysfunction observed so far in ALS could be related to epigenetic mtDNA modifications, as already suggested in Alzheimer's disease [59]. Intriguingly, it was demonstrated that mitochondrial heteroplasmy alters mtDNA methylation [60]. Moreover, a recent study in blood mtDNA of ALS patients, especially from *SOD1* mutation carriers, showed a significant decrease in D-loop methylation accompanied by an increase in mtDNA copy number, the latter representing a mitochondrial compensation for metabolic deregulation caused by oxidative stress in ALS [61]. However, we did not evidence difference in the mtDNA copy number in ALS fibroblasts compared to controls (data not shown). It neither seems likely that the inverse relationship between mtDNA copy number and D-loop methylation in the blood specifically points to ALS; rather, it could point generally to a metabolic imbalance.

## Conclusion

Provided that the discriminant metabolites found in this study are also available in the blood and/or CSF, a collective reading of purine, pyrimidine, arginine, proline metabolites, and DHA-containing lipids could reflects a specific ALS signature. These results in agreement with the ALS research literature, in different affected tissues and body fluids (motor neurons, CSF, blood etc.…), reinforce the interest of fibroblast cultures in the study of ALS. These findings reveal a robust methodology to apply omics, even in subcellular organelles, with data integration with promise to deeply understand ALS pathophysiology. Thus, this approach may be applied to other complex and multifactorial neurological diseases with high confidence.

**Authors' Contributions** C.V-D and H.B designed and supervised the study, performed statistical analysis and wrote the manuscript; C. Br performed mtDNA experiments and analyzed mtDNA sequence; C.V-D and C.Bo performed metabolomic and lipidomic assays, S.C performed cell cultures and mitochondrial function assessment; P.Cod and B.F recruited ALS patients and performed fibroblast sampling; J.C and P. Cou supervised patients' recruitment; P.V supervised genetic determination of genes involved in ALS; R.H gave technical and intellectual support and critical advice for English writing; P.Cor, P.V, and C.R.A gave technical and intellectual support; G.L and P.R gave intellectual support and conceptual advice for manuscript writing. All authors offered conceptual advice and comments on the manuscript. All authors read and approved the final manuscript.

## Compliance with Ethical Standards

**Abbreviations** ALS, amyotrophic lateral sclerosis; sALS, sporadic ALS; ER, endoplasmic reticulum; mtDNA, mitochondrial DNA; PCA, principal component analysis; PLS-DA, partial least square discriminant analysis; OXPHOS, oxidative phosphorylation; FVC, forced vital capacity; BMI, body mass index; HRMS, high-resolution mass spectrometry; UPLC, ultra-performance liquid chromatography; ESI, electrospray ionization; QC, quality control; VIP, variable importance in projection; OCR, oxygen consumption rate; RCR, respiration capacity rate; SM, sphingomyelins; PC, phosphatidylcholines; PE, phosphatidylethanolamines; ROS, reactive oxygen species; CSF, cerebrospinal fluid; Cer, ceramides; DHA, docosahexaenoic acid

## References

1. Korner S, Kollewe K, Ilsemann J, Muller-Heine A, Dengler R, Krampfl K, Petri S (2013) Prevalence and prognostic impact of comorbidities in amyotrophic lateral sclerosis. Eur J Neurol 20(4): 647–654. https://doi.org/10.1111/ene.12015

2. Barber SC, Shaw PJ (2010) Oxidative stress in ALS: key role in motor neuron injury and therapeutic target. Free Radic Biol Med 48(5):629–641. https://doi.org/10.1016/j.freeradbiomed.2009.11.018

3. Guegan C, Vila M, Rosoklija G, Hays AP, Przedborski S (2001) Recruitment of the mitochondrial-dependent apoptotic pathway in amyotrophic lateral sclerosis. J Neurosci 21(17):6569–6576

4. Watanabe M, Dykes-Hoberg M, Culotta VC, Price DL, Wong PC, Rothstein JD (2001) Histological evidence of protein aggregation in mutant SOD1 transgenic mice and in amyotrophic lateral sclerosis neural tissues. Neurobiol Dis 8(6):933–941. https://doi.org/10.1006/nbdi.2001.0443

5. Ferraiuolo L, Kirby J, Grierson AJ, Sendtner M, Shaw PJ (2011) Molecular pathways of motor neuron injury in amyotrophic lateral sclerosis. Nat Rev Neurol 7(11):616–630. https://doi.org/10.1038/nrneurol.2011.152

6. Vandoorne T, De Bock K, Van Den Bosch L (2018) Energy metabolism in ALS: an underappreciated opportunity? Acta Neuropathol 135(4):489–509. https://doi.org/10.1007/s00401-018-1835-x

7. Konrad C, Kawamata H, Bredvik KG, Arreguin AJ, Cajamarca SA, Hupf JC, Ravits JM, Miller TM et al (2017) Fibroblast bioenergetics to classify amyotrophic lateral sclerosis patients. Mol Neurodegener 12(1):76. https://doi.org/10.1186/s13024-017-0217-5

8. Walczak J, Debska-Vielhaber G, Vielhaber S, Szymanski J, Charzynska A, Duszynski J, Szczepanowska J (2018) Distinction of sporadic and familial forms of ALS based on mitochondrial characteristics. Faseb j:fj201801843R. doi:https://doi.org/10.1096/fj.201801843R

9. Allen SP, Duffy LM, Shaw PJ, Grierson AJ (2015) Altered age-related changes in bioenergetic properties and mitochondrial morphology in fibroblasts from sporadic amyotrophic lateral sclerosis patients. Neurobiol Aging 36(10):2893–2903. https://doi.org/10.1016/j.neurobiolaging.2015.07.013

10. Allen SP, Rajan S, Duffy L, Mortiboys H, Higginbottom A, Grierson AJ, Shaw PJ (2014) Superoxide dismutase 1 mutation in a cellular model of amyotrophic lateral sclerosis shifts energy generation from oxidative phosphorylation to glycolysis. Neurobiol Aging 35(6):1499–1509. https://doi.org/10.1016/j.neurobiolaging.2013.11.025

11. Kirk K, Gennings C, Hupf JC, Tadesse S, D'Aurelio M, Kawamata H, Valsecchi F, Mitsumoto H et al (2014) Bioenergetic markers in skin fibroblasts of sporadic amyotrophic lateral sclerosis and progressive lateral sclerosis patients. Ann Neurol 76(4):620–624. https://doi.org/10.1002/ana.24244

12. Fonteh AN, Fisher RD (2009) Combining lipidomics and proteomics of human cerebrospinal fluids. Methods Mol Biol 579:71–86. https://doi.org/10.1007/978-1-60761-322-0_4

13. Puentes F, Malaspina A, van Noort JM, Amor S (2016) Non-neuronal cells in ALS: Role of glial, immune cells and blood-CNS barriers. Brain Pathol 26(2):248–257. https://doi.org/10.1111/bpa.12352

14. Szymanski J, Janikiewicz J, Michalska B, Patalas-Krawczyk P, Perrone M, Ziolkowski W, Duszynski J, Pinton P et al (2017) Interaction of mitochondria with the endoplasmic reticulum and plasma membrane in calcium homeostasis, lipid trafficking and mitochondrial structure. Int J Mol Sci 18(7). https://doi.org/10.3390/ijms18071576

15. Kaus A, Sareen D (2015) ALS patient stem cells for unveiling disease signatures of motoneuron susceptibility: perspectives on the deadly mitochondria, ER stress and calcium triad. Front Cell Neurosci 9:448. https://doi.org/10.3389/fncel.2015.00448

16. Turner BJ, Atkin JD (2006) ER stress and UPR in familial amyotrophic lateral sclerosis. Curr Mol Med 6(1):79–86

17. Ilieva EV, Ayala V, Jove M, Dalfo E, Cacabelos D, Povedano M, Bellmunt MJ, Ferrer I et al (2007) Oxidative and endoplasmic reticulum stress interplay in sporadic amyotrophic lateral sclerosis. Brain 130(Pt 12):3111–3123. https://doi.org/10.1093/brain/awm190

18. Veyrat-Durebex C, Bocca C, Chupin S, Kouassi Nzoughet J, Simard G, Lenaers G, Reynier P, Blasco H (2018) Metabolomics and lipidomics profiling of a combined mitochondrial plus endoplasmic reticulum fraction of human fibroblasts: a robust tool for clinical studies. J Proteome Res 17(1):745–750. https://doi.org/10.1021/acs.jproteome.7b00637

19. Aviram R, Manella G, Kopelman N, Neufeld-Cohen A, Zwighaft Z, Elimelech M, Adamovich Y, Golik M et al (2016) Lipidomics analyses reveal temporal and spatial lipid organization and uncover daily oscillations in intracellular organelles. Mol Cell 62(4):636–648. https://doi.org/10.1016/j.molcel.2016.04.002

20. Kappler L, Li J, Haring HU, Weigert C, Lehmann R, Xu G, Hoene M (2016) Purity matters: a workflow for the valid high-resolution lipid profiling of mitochondria from cell culture samples. Sci Rep 6: 21107. doi:https://doi.org/10.1038/srep21107

21. Bird SS, Stavrovskaya IG, Gathungu RM, Tousi F, Kristal BS (2015) Qualitative characterization of the rat liver mitochondrial lipidome using all ion fragmentation on an Exactive benchtop Orbitrap MS. Methods Mol Biol 1264:441–452. https://doi.org/10.1007/978-1-4939-2257-4_36

22. Angelini R, Vitale R, Patil VA, Cocco T, Ludwig B, Greenberg ML, Corcelli A (2012) Lipidomics of intact mitochondria by MALDI-TOF/MS. J Lipid Res 53(7):1417–1425. https://doi.org/10.1194/jlr.D026203

23. Brooks BR, Miller RG, Swash M, Munsat TL (2000) El Escorial revisited: revised criteria for the diagnosis of amyotrophic lateral sclerosis. Amyotroph Lateral Scler Other Motor Neuron Disord 1(5):293–299

24. Hutter E, Renner K, Pfister G, Stockl P, Jansen-Durr P, Gnaiger E (2004) Senescence-associated changes in respiration and oxidative phosphorylation in primary human fibroblasts. The Biochem J 380 (Pt 3):919–928. doi:https://doi.org/10.1042/bj20040095

25. Bocca C, Kane MS, Veyrat-Durebex C, Chupin S, Alban J, Kouassi Nzoughet J, Le Mao N, Chao de la Barca JM et al (2018) The metabolomic bioenergetic signature of Opa1-disrupted mouse embryonic fibroblasts highlights aspartate deficiency. Sci Rep 8(1): 11528. https://doi.org/10.1038/s41598-018-29972-9

26. Sumner LW, Amberg A, Barrett D, Beale MH, Beger R, Daykin CA, Fan TW, Fiehn O et al (2007) Proposed minimum reporting standards for chemical analysis chemical analysis working group (CAWG) metabolomics standards initiative (MSI). Metabolomics 3(3):211–221. https://doi.org/10.1007/s11306-007-0082-2

27. Boucret L, Bris C, Seegers V, Goudenege D, Desquiret-Dumas V, Domin-Bernhard M, Ferre-L'Hotellier V, Bouet PE et al (2017) Deep sequencing shows that oocytes are not prone to accumulate mtDNA heteroplasmic mutations during ovarian ageing. Hum Reprod 32(10):2101–2109. https://doi.org/10.1093/humrep/dex268

28. Robinson JT, Thorvaldsdottir H, Winckler W, Guttman M, Lander ES, Getz G, Mesirov JP (2011) Integrative genomics viewer. In: Nat Biotechnol, vol 29. vol 1. United States, pp 24–26. doi:https://doi.org/10.1038/nbt.1754

29. Lott MT, Leipzig JN, Derbeneva O, Xie HM, Chalkia D, Sarmady M, Procaccio V, Wallace DC (2013) mtDNA variation and analysis using Mitomap and Mitomaster. Curr Protoc Bioinformatics 44: 1.23.21–1.23.26. https://doi.org/10.1002/0471250953.bi0123s44

30. Clima R, Preste R, Calabrese C, Diroma MA, Santorsola M, Scioscia G, Simone D, Shen L et al (2017) HmtDB 2016: data update, a better performing query system and human mitochondrial DNA haplogroup predictor. Nucleic Acids Res 45(D1):D698–d706. https://doi.org/10.1093/nar/gkw1066

31. Putz J, Dupuis B, Sissler M, Florentz C (2007) Mamit-tRNA, a database of mammalian mitochondrial tRNA primary and secondary structures. RNA (New York, NY) 13(8):1184–1190. https://doi.org/10.1261/rna.588407

32. Castellana S, Ronai J, Mazza T (2015) MitImpact: an exhaustive collection of pre-computed pathogenicity predictions of human mitochondrial non-synonymous variants. Hum Mutat 36(2):E2413–E2422. https://doi.org/10.1002/humu.22720

33. Sonney S, Leipzig J, Lott MT, Zhang S, Procaccio V, Wallace DC, Sondheimer N (2017) Predicting the pathogenicity of novel variants in mitochondrial tRNA with MitoTIP. PLoS Comput Biol 13(12): e1005867. https://doi.org/10.1371/journal.pcbi.1005867

34. Navarro-Gomez D, Leipzig J, Shen L, Lott M, Stassen AP, Wallace DC, Wiggs JL, Falk MJ, van Oven M, Gai X (2015) Phy-Mer: a novel alignment-free and reference-independent mitochondrial haplogroup classifier. Bioinformatics 31(8):1310–1312. https://doi.org/10.1093/bioinformatics/btu825

35. Madji Hounoum B, Mavel S, Coque E, Patin F, Vourc'h P, Marouillat S, Nadal-Desbarats L, Emond P et al (2017) Wildtype motoneurons, ALS-linked SOD1 mutation and glutamate profoundly modify astrocyte metabolism and lactate shuttling. Glia 65(4):592–605. https://doi.org/10.1002/glia.23114

36. Volonte C, Apolloni S, Parisi C, Amadio S (2016) Purinergic contribution to amyotrophic lateral sclerosis. Neuropharmacology 104: 180–193. https://doi.org/10.1016/j.neuropharm.2015.10.026

37. Angermuller S, Islinger M, Volkl A (2009) Peroxisomes and reactive oxygen species, a lasting challenge. Histochem Cell Biol 131(4):459–463. https://doi.org/10.1007/s00418-009-0563-7

38. Ames BN, Cathcart R, Schwiers E, Hochstein P (1981) Uric acid provides an antioxidant defense in humans against oxidant- and radical-caused aging and cancer: a hypothesis. Proc Natl Acad Sci U S A 78(11):6858–6862

39. Sautin YY, Johnson RJ (2008) Uric acid: the oxidant-antioxidant paradox. Nucleosides, Nucleotides Nucleic Acids 27(6):608–619. https://doi.org/10.1080/15257770802138558

40. Fang P, Li X, Luo JJ, Wang H, Yang XF (2013) A double-edged sword: uric acid and neurological disorders. Brain Disord Ther 2(2): 109. https://doi.org/10.4172/2168-975x.1000109

41. Huang TT, Hao DL, Wu BN, Mao LL, Zhang J (2017) Uric acid demonstrates neuroprotective effect on Parkinson's disease mice through Nrf2-ARE signaling pathway. Biochem Biophys Res Commun 493(4):1443–1449. https://doi.org/10.1016/j.bbrc.2017.10.004

42. Bakshi R, Xu Y, Mueller KA, Chen X, Granucci E, Paganoni S, Sadri-Vakili G, Schwarzschild MA (2018) Urate mitigates oxidative stress and motor neuron toxicity of astrocytes derived from ALS-linked SOD1(G93A) mutant mice. Mol Cell Neurosci 92: 12–16. https://doi.org/10.1016/j.mcn.2018.06.002

43. Lazzarino G, Amorini AM, Petzold A, Gasperini C, Ruggieri S, Quartuccio ME, Di Stasio E, Tavazzi B (2017) Serum compounds of energy metabolism impairment are related to disability, disease course and neuroimaging in multiple sclerosis. Mol Neurobiol 54(9):7520–7533. https://doi.org/10.1007/s12035-016-0257-9

44. Persky AM, Brazeau GA (2001) Clinical pharmacology of the dietary supplement creatine monohydrate. Pharmacol Rev 53(2): 161–176

45. Li H, Tang Z, Chu P, Song Y, Yang Y, Sun B, Niu M, Qaed E et al (2018) Neuroprotective effect of phosphocreatine on oxidative stress and mitochondrial dysfunction induced apoptosis in vitro and in vivo: Involvement of dual PI3K/Akt and Nrf2/HO-1 pathways. Free Radic Biol Med 120:228–238. https://doi.org/10.1016/j.freeradbiomed.2018.03.014

46. Vallee A, Lecarpentier Y, Guillevin R, Vallee JN (2018) Aerobic glycolysis in amyotrophic lateral sclerosis and Huntington's disease. Rev Neurosci 29(5):547–555. https://doi.org/10.1515/revneuro-2017-0075

47. Lu W, Su X, Klein MS, Lewis IA, Fiehn O, Rabinowitz JD (2017) Metabolite measurement: pitfalls to avoid and practices to follow. Annu Rev Biochem 86:277–304. https://doi.org/10.1146/annurev-biochem-061516-044952

48. Farooqui AA, Horrocks LA (2001) Plasmalogens, phospholipase A2, and docosahexaenoic acid turnover in brain tissue. J Mol Neurosci 16(2–3):263–272 discussion 279–284

49. Peters OM, Ghasemi M, Brown RH Jr (2015) Emerging mechanisms of molecular pathology in ALS. J Clin Invest 125(6):2548. https://doi.org/10.1172/jci82693

50. Luoma AM, Kuo F, Cakici O, Crowther MN, Denninger AR, Avila RL, Brites P, Kirschner DA (2015) Plasmalogen phospholipids protect internodal myelin from oxidative damage. Free Radic Biol Med 84:296–310. https://doi.org/10.1016/j.freeradbiomed.2015.03.012

51. Sindelar PJ, Guan Z, Dallner G, Ernster L (1999) The protective role of plasmalogens in iron-induced lipid peroxidation. Free Radic Biol Med 26(3–4):318–324

52. Blasco H, Veyrat-Durebex C, Bocca C, Patin F, Vourc'h P, Kouassi Nzoughet J, Lenaers G, Andres CR et al (2017) Lipidomics reveals cerebrospinal-fluid signatures of ALS. Sci Rep 7(1):17652. https://doi.org/10.1038/s41598-017-17389-9

53. Dodge JC, Treleaven CM, Pacheco J, Cooper S, Bao C, Abraham M, Cromwell M, Sardi SP et al (2015) Glycosphingolipids are modulators of disease pathogenesis in amyotrophic lateral sclerosis. Proc Natl Acad Sci U S A 112(26):8100–8105. https://doi.org/10.1073/pnas.1508767112

54. Ariga T, Jarvis WD, Yu RK (1998) Role of sphingolipid-mediated cell death in neurodegenerative diseases. J Lipid Res 39(1):1–16

55. Henriques A, Croixmarie V, Priestman DA, Rosenbohm A, Dirrig-Grosch S, D'Ambra E, Huebecker M, Hussain G et al (2015) Amyotrophic lateral sclerosis and denervation alter sphingolipids and up-regulate glucosylceramide synthase. Hum Mol Genet 24(25):7390–7405. https://doi.org/10.1093/hmg/ddv439

56. Arima H, Hanada M, Hayasaka T, Masaki N, Omura T, Xu D, Hasegawa T, Togawa D et al (2014) Blockade of IL-6 signaling by MR16-1 inhibits reduction of docosahexaenoic acid-containing phosphatidylcholine levels in a mouse model of spinal cord injury. Neuroscience 269:1–10. https://doi.org/10.1016/j.neuroscience.2014.03.012

57. Akbar M, Calderon F, Wen Z, Kim HY (2005) Docosahexaenoic acid: a positive modulator of Akt signaling in neuronal survival. Proc Natl Acad Sci U S A 102(31):10858–10863. https://doi.org/10.1073/pnas.0502903102

58. Hong S, Gronert K, Devchand PR, Moussignac RL, Serhan CN (2003) Novel docosatrienes and 17S-resolvins generated from docosahexaenoic acid in murine brain, human blood, and glial cells. Autacoids in anti-inflammation. J Biol Chem 278(17):14677–14687. https://doi.org/10.1074/jbc.M300218200

59. Devall M, Mill J, Lunnon K (2014) The mitochondrial epigenome: a role in Alzheimer's disease? Epigenomics 6(6):665–675. https://doi.org/10.2217/epi.14.50

60. Hua S, Lu C, Song Y, Li R, Liu X, Quan F, Wang Y, Liu J et al (2012) High levels of mitochondrial heteroplasmy modify the development of ovine-bovine interspecies nuclear transferred embryos. Reprod Fertil Dev 24(3):501–509. https://doi.org/10.1071/rd11091

61. Stoccoro A, Mosca L, Carnicelli V, Cavallari U, Lunetta C, Marocchi A, Migliore L, Coppede F (2018) Mitochondrial DNA copy number and D-loop region methylation in carriers of amyotrophic lateral sclerosis gene mutations. Epigenomics 10:1431–1443. https://doi.org/10.2217/epi-2018-0072